Journal of Chemical Neuroanatomy 129 (2023) 102256

Contents lists available at ScienceDirect

Journal of Chemical Neuroanatomy

journal homepage: www.elsevier.com/locate/jchemneu

Polyoxidovanadates as a pharmacological option against brain aging

Alfonso Díaz [b,1], Rubén Vázquez-Roque [c,2], Karen Carreto-Meneses [a,3], Diana Moroni-González [a,4], José Albino Moreno-Rodríguez [a], Samuel Treviño [a,5,*]

[a] Laboratory of Chemical-Clinical Investigations, Department of Clinical Chemistry, Faculty of Chemistry Science, University Autonomous of Puebla, 14 South. FCQ1, University City, Puebla C.P. 72560, Mexico
[b] Department of Pharmacy, Faculty of Chemistry Science, University Autonomous of Puebla, 22 South. FC91, University City, Puebla C.P. 72560, Mexico
[c] Neuropsychiatry laboratory, Physiology Institute, University Autonomous of Puebla, 14 South. University City, Puebla C.P. 72560, Mexico

ARTICLE INFO

Keywords:
Aging
Hippocampi
Inflammaging
Oxidative stress
Polyoxidovanadates, Metforminium-decavanadate

ABSTRACT

The world population is aging rapidly, and chronic diseases associated are cardiometabolic syndrome, cancer, and neurodegenerative diseases. Oxidative stress and inflammation are typical hallmarks in them. Polyoxidovanadates (POVs) have shown interesting pharmacological actions against chronic diseases. This work aimed to evaluate the POV effect on hippocampal neuroinflammation, redox balance, and recognition memory in the aging of rats. Rats 18 months old were administered a daily dose of sodium metavanadate (MV), decavanadate (DV), Metformin (Metf), or MetfDeca for two months. Results showed that short-term and long-term recognition memory improved by 28 % and 16 % (DV), 19 % and 20 % (Metf), and 21 % and 27 % (MetfDeca). In hippocampi, reactive oxygen species, IL-1β, and TNF-α, after DV, Metf, and MetfDeca decreased at similar concentrations to young adult control, while lipid peroxidation substantially ameliorated. Additionally, superoxide dismutase and catalase activity increased by 41 % and 42 % (DV), 39 % and 41 % (Metf), and 75 % and 73 % (MetfDeca). POV treatments reduced Nrf2 and GFAP immunoreactivity in CA1 (70–87.5 %), CA3 (60–80 %), and DG (57–89 %). Metformin treatment showed a minor effect, while MV treatment did not improve any parameters. Although DV, Metf, and MetfDeca treatments showed similar results, POVs doses were 16-fold fewer than Metformin. In conclusion, DV and MetfDeca could be pharmacological options to reduce age-related neuronal damage.

1. Introduction

The world population is aging rapidly. United Nations established in 2019 that 703 million people aged 65 or older are in the global population. The projection for 2050 is 1.5 billion, almost 22 % of the worldwide population (Foroushani et al., 2014; Nations Department of Economic, 2019). The aging process leads to indiscriminate loss of physiological functions across an organism because of reduced reparative and regenerative potential in tissues and organs, allowing degenerative diseases to appear (Khan et al., 2017). The chronic diseases observed in aging are cardiovascular disease, cancer, osteoporosis, arthritis, and diabetes, and the main two neurodegenerative diseases are Alzheimer's and Parkinson's (Khan et al., 2017; Mattson and Arumugam, 2018; Perry et al., 2018).

During aging, many people lose the capacity for learning and memory, attention, decision-making speed, sensory perception, and motor coordination (Alexander et al., 2012; Dykiert et al., 2012; Levin et al., 2014). Several studies have demonstrated an overall reduction in brain volume, with most of the gray matter shrinkage occurring in the prefrontal cortex and hippocampus, which are critical areas for various complex cognitive processes (Flores et al., 2020, 2016; Isaev et al., 2019; Wahl et al., 2019). The brain is highly metabolically active, using nearly

* Correspondence to: Laboratory of Chemical-Clinical Investigations, Department of Clinical Chemistry, Faculty of Chemistry Science, Benemérita Universidad Autónoma de Puebla, 14 Sur. FCQ1, Ciudad Universitaria, Puebla C.P. 72560, Mexico.
E-mail address: samuel.trevino@correo.buap.mx (S. Treviño).
[1] 0000–0003-4092–6636
[2] 0000–0002-2712–5714
[3] 0000–0003-3812–3535
[4] 0000–0003-4500–0648
[5] 0000–0001-5679–1671

https://doi.org/10.1016/j.jchemneu.2023.102256
Received 26 October 2022; Received in revised form 10 March 2023; Accepted 11 March 2023
Available online 13 March 2023

a quarter of the body's total glucose and oxygen consumption. The high level of oxygen consumption can lead to an increase in the production of reactive oxygen species (ROS). As set out by the free radical and mitochondrial dysfunction theories of aging, increased ROS could result in oxidative damage and inflammation, which are redundant and progressive (Barja, 2014, 2013; Sanz and Stefanatos, 2010). Therefore, the pharmacological strategies must be focused on developing molecules with a broad spectrum of activity that positively impacts deleterious mechanisms of brain aging.

In the last 30 years, the number of studies of polyoxidometalates (POMs), and particularly polyoxidovanadates (POVs) such as decavanadate and related compounds, have been associated with enzymatic inhibition, insulin signaling enhancement, improvement of dysglycemia and dyslipidemia, and inhibition of the aggregation of amyloid β-peptides related to Alzheimer's disease (Fig. 1) (Aureliano, 2022, 2016, 2011; Aureliano et al., 2022). Decavanadate, $[V_{10}O_{28}]^{6-}$ is an isopolyoxidovanadate described in detail and showcases the relevance of POV speciation and stability to exert biological effects (Aureliano et al., 2022). Decavanadate is stable for weeks in pure aqueous at pH 4.0, and no change in the hydrolysis rate is observed (Aureliano et al., 2016). Our workgroup has informed that the chimeric compound metforminium decavanadate $(H_2Metf)_3[V_{10}O_{28}]\bullet 8\ H_2O$ (MetfDeca) has pharmacological potential as a hypoglycemic, lipid-lowering, and metabolic regulator since the resulting compound is made of the two components with antidiabetic activities that reduce both dosages (48,000 times) and time of administration (twice a week) (Treviño et al., 2016, 2015). MetfDeca is an effective treatment against insulin resistance, metabolic syndrome, and type 1 and type 2 diabetes, with a protective effect on pancreatic beta cells (Treviño et al., 2019, 2018). MetfDeca ameliorated oxidative stress, redox balance, and insulin signaling in the liver and muscle of animals with type 1 diabetes (Treviño and González-Vergara, 2019). Recently, we observed that MetfDeca reduced oxidative stress and hippocampal neuroinflammation in rats with metabolic syndrome, increased the density and length of the dendritic spines of the hippocampus, and restored spatial and recognition memory (Diaz et al., 2021).

The expected effects of brain aging are lost neural function, where reactive astrogliosis increases oxidative stress and pro-inflammatory cytokines (at least in part), modulating transcriptional regulation of nuclear factor erythroid 2-related factor 2 (Nrf2), a master sensor of redox balance (Zhou et al., 2019). Nrf2 activation positively regulates the expression of enzymes and peptides anti-oxidative that avoid neurodegeneration. In the liver and muscle of diabetic rats treated with MetfDeca, redox balance improved and was associated with an Nrf2 increase (Treviño and González-Vergara, 2019). Metformin and POVs such as MetfDeca and decavanadate ameliorate cell functions, inflammation, and balance redox (Silva-Nolasco et al., 2020). Therefore, in this study, we aimed to evaluate the effect of vanadium compounds and Metformin on hippocampal neuroinflammation, redox balance, and recognition memory in aged rats.

2. Materials and methods

Male Wistar rats of 2 months (n = 8) and 18 months (n = 40) were used. The "Claude Bernard" Animal Facility of the University of Puebla provided the animals. The rats were housed in acrylic boxes at controlled temperature and humidity, with light-dark cycles of 12 h each, with free access to water and food. The diet used was LabDiet 5001 (Laboratory Rodent Diet); its composition can be consulted on the manufacturer's website. The procedures described in this study were carried out following the Standards for the Use and Care of Laboratory Animals defined by the Mexican Council for Animal Care (NOM-062-ZOO-1999), as well as the Guide of the National Institutes of Health for the Care and Use of Laboratory Animals, and the Ethics Committee of the Autonomous University of Puebla. In this study, every effort was made to minimize animal suffering. The number of animals in the current study is small, as the subjects were 18 months old. If signs of distress appeared in the animals before or during the experimentation, a veterinarian immediately evaluated them.

2.1. Pharmacological treatments

Five experimental groups were designated for this study (n = 8/group): (1) control young adult (drinking water: 1 mL/kg); (2) control aging (drinking water: 1 mL/kg); (3) sodium metavanadate (MV; 1.23 μg/0.1 kg); (4) Decavanadate (DV; 1.23 μg/0.1 kg); (5) Metformin (Metf; 200 mg/kg), and (6) MetfDeca (1.23 μg/0.1 kg). All treatments were dissolved in 1 mL of drinking water, adjusted to weight, and administered by oral gavage for 60 days between 8:00 and 10:00 am. Groups 1 and 2 (controls) were administered 1 mL of drinking water in identical conditions. Treatment doses of each drug were selected based on published reports (Diaz et al., 2021; Muñoz-Arenas et al., 2020; Treviño et al., 2018, 2016).

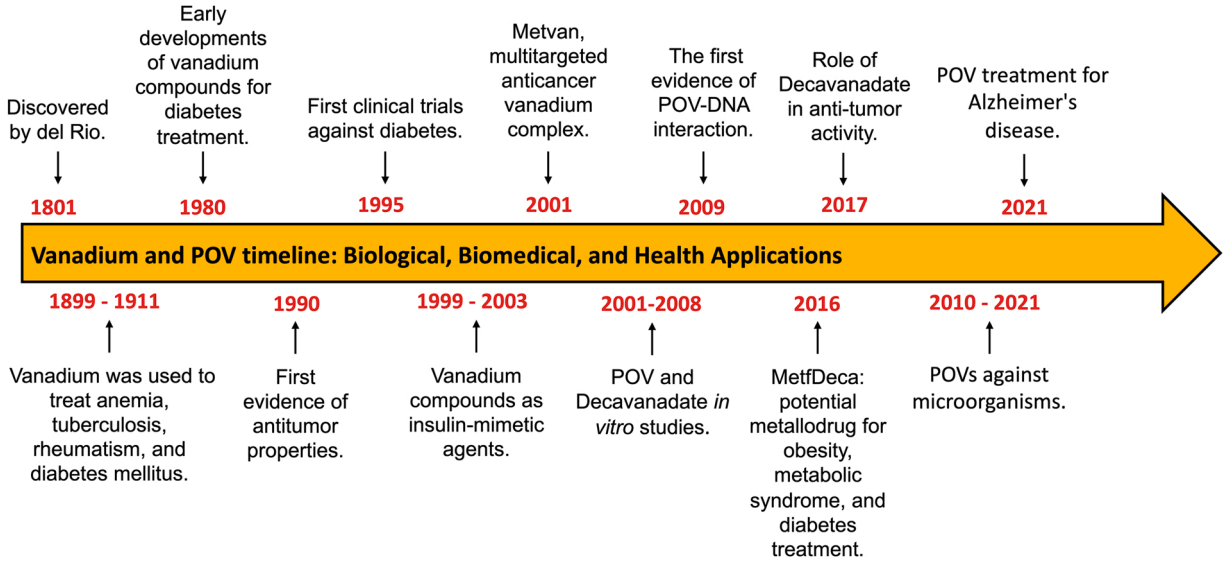

Fig. 1. POVs Biological, Biomedical, and Health Applications.

2.2. Novel Object Recognition Test (NORt)

The methodology NORt employed is described by Diaz et al., which evaluates the recognition memory (Diaz et al., 2021). The test is based on quantifying the time required for animals to explore a novel object compared to a familiar object (Muñoz-Arenas et al., 2020). The animals were placed in a dark plastic box four times (80 cm wide X 80 cm long X 80 cm high). Four plastic objects of different colors and sizes (width = 9.0–12.0 cm, height = 6.0–9.0 cm) were used for this test. The objects were located on the box floor, diagonally and opposite, at a distance of ~30 cm. The NORt was recorded with a video camera attached to the wall above the box. The lighting of the box was made of white light. Animals were acclimatized for 45 min three days before the test.

Habituation is the first phase of the NORt. Rats scanned the empty box for 5 min and returned to their cage. In this phase, the distance traveled (cm) by the animals of each experimental group was analyzed and graphed. Twenty-four hours after the habituation phase ended, the animals performed the familiarization phase. The rats were placed in the center of the box with two identical objects. The scan time for each object was quantified for 5 min from when the nose of the rat was 1 cm to the object and the animal's vibrissae moved. The short-term recognition memory (STRM) was evaluated as follows, one of the similar objects (familiar object) previously placed in the box in the familiarization phase was replaced by a new one (novel object). Subsequently, the rats were placed in the center of the box for 5 min. The exploration time for each object was recorded similarly to the familiarization phase. The preference for exploring the novel object was determined by the time a rat spent exploring the new object compared to the familiar object. Long-term recognition memory (LTMR) was evaluated 24 h after performing the STRM. In this phase, the previously presented object as a novelty in the STRM was replaced by a new object to evaluate the LTMR, as described in the familiarization phase. In both the STRM and LTRM, the discrimination index (DI) = (TN - TF) / (TN + TF) was determined, identifying TF and TN as the time to explore familiar and new objects. After each session, the box and objects were cleaned with 80 % ethanol to exclude odor signals.

2.3. Samples for biochemical tests

After finishing the NORT, four animals from each group were decapitated. Then, the brains were extracted, and the hippocampus (Hp) was dissected at the level of the anterior temporal area approximately 3.8–6.8 mm from the bregma, taking the rat brain in stereotaxic coordinates atlas as a reference (Liang et al., 2017). The tissue was homogenized in 3 mL of frozen phosphate buffer (0.1 M; pH 7.4). The homogenate was centrifuged at 12,500 rpm for 30 min and at 4 °C. The supernatant was obtained and stored at − 70 °C. The supernatant was used to quantify reactive oxygen species (ROS), lipid peroxidation (LPO), pro-inflammatory cytokines, and the activity of superoxide dismutase (SOD) and catalase (CAT).

2.4. Reactive oxygen species assay

Five μL of each homogenate was used. A solution of TRIS, 2- (4- (2-Hydroxyethyl) piperazin-1-yl) ethanesulfonic acid (HEPES) [40 mM] and 2′7'-dichlorodihydrofluorescein diacetate (DCFHDA) [5 μM] was added. The mixes were incubated at 37 °C for 1 h. Subsequently, the sample was analyzed in a luminescence spectrometer (PerkinElmer LS50-B) at 488 nm of excitation and 525 nm of emission wavelength. The respective values of each sample were determined from a standard curve of 2′7′-dichlorofluorescein (DCF) (Sigma-Aldrich). The results were expressed in nanomoles of DFC per mg of protein (Diaz et al., 2021).

2.5. Lipid peroxidation assay

One mL of the supernatant of each tissue was mixed with 4 mL of chloroform-methanol (2:1, v/v). The samples were allowed to stand at 4 °C in the dark for 1 h. The oily phase was removed, and the aqueous phase was excited at a wavelength of 370 nm; the emission obtained at 430 nm was on a PerkinElmer LS50-B luminescence spectrometer at 25 °C. The sensitivity of the equipment was adjusted to a fluorescent signal of 140 fluorescence units (FU) with the help of a standard solution of quinine (0.001 mg / mL) and H_2SO_4 (0.05 M). The results were expressed as relative fluorescence units (RFU) per milligram of protein (Diaz et al., 2021).

2.6. Quantification of IL-1 β and TNF-α

The IL-1β and TNF-α concentration in the brain samples was quantified employing a sandwich immunoassay (R&D Systems, Minneapolis, MN). The absorbance was proportionally related to the amount of each of the cytokines. The lower detection limits for each ELISA technique were 0.7 and 1.0 pg/mg of protein for IL-1β and TNF-α, respectively.

2.7. Superoxide dismutase and catalase activity assay

The pyrogallol method was used to evaluate SOD activity. A Tris-HCl (0.05 M, pH 8.2) solution with Na_2EDTA (1 mM) was placed in a quartz cell. A mixture of 50 μL of pyrogallol (12 mM in 1 mM HCl) and 50 μL of the hippocampal supernatant was vigorously shaken. The reaction was monitored every 30 s for 5 min in a Lambda EZ-150 spectrophotometer (PerkinElmer Company) at 420 nm and room temperature. The SOD activity was obtained, considering that 1 U is the amount of enzyme that inhibits the autooxidation of pyrogallol by 50 % at 25 °C and pH 8.2.

The CAT activity was performed in a spectrophotometer (Lambda EZ-150, PerkinElmer Company). The samples (50 μL) were mixed with 20 mM of a potassium phosphate buffer solution (50 mM at pH 7.0; 1:20 dilution) and subsequently centrifuged at 10,000g/10 min/4 °C. The technique included mixing 2.0 mL of potassium phosphate buffer solution, 0.05 mL of H_2O_2 (0.3 M), and 50 μL of the sample. Then the H_2O_2 decomposition was followed for 60 s at 240 nm. Catalase activity was calculated as μmol / min / mg protein, equivalent to U/mg protein.

Proteins were quantified according to the Lowry method. A calibration curve from 5 to 150 μg/μL of albumin was prepared, 20 μL of the curve or an aliquot of the homogenates was mixed with 100 μL of 0.1 N sodium hydroxide, 1.5 mL of alkaline solution ($KNaC_4H_4O_6 \bullet 4\ H_2O$ 2 % and $CuSO_4$ 1 % in 0.1 N NaOH), and 200 μL of Folin reagent. The solutions were incubated for 10 min at 37 °C, and the absorbance was read at 500 nm. The concentration in the samples was calculated by extrapolation with the albumin curve.

2.8. Immunohistochemistry

After behavioral testing, rats (n = 4 / group) were anesthetized with sodium pentobarbital (40 mg/kg, i.p.) and perfused intracardially with PBS and paraformaldehyde (4 %). The brains were post-fixed overnight at 4 °C. After the fixation time, the tissues were placed in a histokinet automatic tissue processor (Leica TP1020) to be dehydrated with ethanol in increasing percentages until 100%. Subsequently, the brains were rinsed with Xylol and submerged in liquid paraffin (50 °C) for infiltration. Finally, the tissues were placed coronally in embedding molds (Matrix Laboratories, 30 × 24 × 5 mm) to generate paraffin blocks.

Tissue Section 5-μm thick were taken from each tissue. Paraffin was removed, and the tissues were rehydrated. Tissue was incubated in 2 % IgG-free bovine serum albumin (BSA, Sigma, USA) to block non-specific binding sites. Then, the samples were permeated with 0.2 % Triton X-100 and subsequently incubated overnight at 4 °C with primary antibodies, Glial Fibrillary Acidic Protein (GFAP; 1:1000, Millipore Ab7260)

as a marker for astrocytes and Nuclear factor erythroid 2-related factor 2 (Nrf2, sc-722; 1:50, Santa Cruz Biotechnology Inc., CA, USA), which were followed by FITC-labeled anti-rabbit secondary antibodies (1:100, Jackson Immuno Research Laboratories Inc.; green channel). The slides were coverslipped in VectaShield medium with DAPI (Vector Labs., CA) for nuclear staining (blue channel). Photomicrographs were taken in a fluorescence microscope (Leica Microsystems GmbH, Wetzlar, Germany) and projected with a Leica IM1000 version 1.20 release-9 computer-based program (Imagic Bildverarbeitung AG, Leica Microsystems, Heerbrugg, Switzerland).

Three consecutive slices of each brain tissue were used to observe the *cornu ammonis* (CA)− 1, − 3, and dentate gyrus (DG) regions of the hippocampal neurons at 40X. The immunoreactive number of cells for each of the antibodies was counted. The criteria to define reactive astrocytes included high immunoreactivity for GFAP, denoting soma and branch extension. Meanwhile, Nrf2 immunoreactivity was detected around the nucleus and cytoplasm of hippocampal cells. The scale bar was adjusted to 30 μm. Five fields per slide (185 μm × 135 μm) were analyzed and expressed graphically as average per group ± standard error of the mean (SEM). All count measurements were performed by a morphology specialist who was unaware of the particularities of the study.

2.9. Statistical analysis

A Shapiro-Wilk normality test was performed to verify that the different data come from a normally distributed population. The results were expressed as the mean ± SEM for all experiments. The results were analyzed by a Two-way ANOVA followed by a Bonferroni test, where $p < 0.05$ was considered significant. Data were analyzed using GraphPad Prism 9.0 (GraphPad Software Inc., USA). Two-way ANOVA analyzed treatment's interaction on aging as independent variables; only significant F statistics are discussed.

3. Results

3.1. Decavanadate compounds improve object recognition memory

The data showed that the distance covered by the control young adult group was 1463 ± 52.4 cm, while the control aging group was 1100 ± 25.3 cm, and the rats of the MV group registered an average of 1010 ± 26 cm. The DV, Metf, and MetfDeca groups walked a distance of 1226 ± 143 cm, 1286 ± 34 cm, and 1172 ± 34 cm, respectively. The covered distance between treated groups was statistically different than the control young adult group ($P < 0.0001$; $F = 29.04$), but they were not different from the control aging group ($P = 0.5225$; $F = 8.71$; Fig. 2A).

The animals were placed in a box with two identical objects in the familiarization phase. The objective was to quantify the time that the animals of each group explored similar objects for 5 min. The data revealed that the mean exploration time was as follows, control young adult by 36.4 ± 1 s; control aging by 26.0 ± 1 s; MV by 27.4 ± 2 s; DV by 27.8 ± 1 s; Metf by 28.0 ± 1 s, and MetfDeca by 29.0 ± 1 s (Fig. 2B). Statistical analysis showed significative difference regarding control

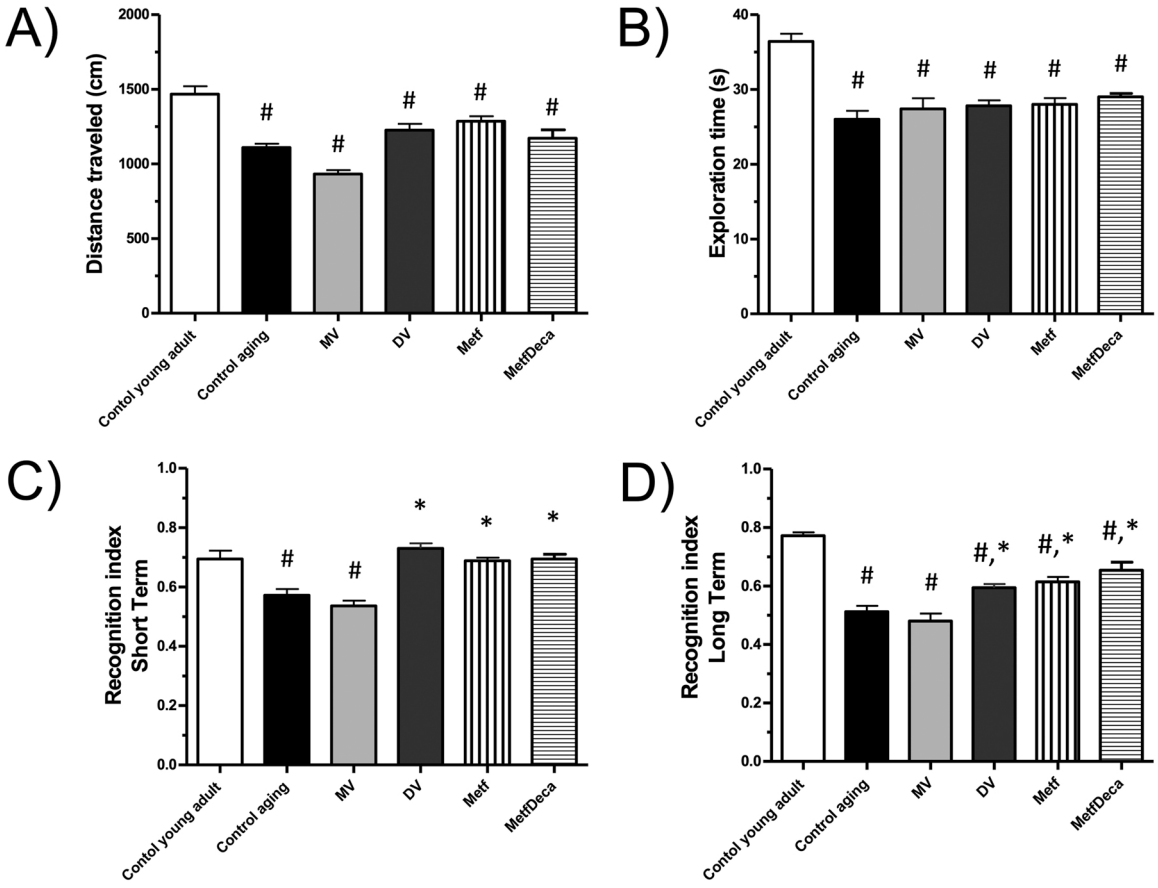

Fig. 2. Treatment with MetfDeca improves recognition memory in rats aging. The NORt was performed by (1) Control young adult; (2) Control aging; (3) MV (metavanadate); (4) DV (decavanadate); (5) Metf (Metformin); and (6) MetfDeca. Data are reported as mean ± standard error of the mean (SEM; n = 8 per group). (a) Distance traveled; (b) Exploration time; (c) recognition index (STRM); and (d) recognition memory (LTRM). A two-way ANOVA test was used to analyze the vanadium treatment interaction on aging as independent variables, and a Bonferroni post-test was used to analyze significant differences ($P < 0.05$). (*) Indicates significant differences from the control aging group. (#) Significant differences from the control young adult group.

young adult ($P < 0.0001$; $F = 18.33$), but they not from the control aging group ($P = 0.7987$; $F = 3.46$).

The recognition indexes were recorded in the third phase to evaluate the STMR and LTMR. At this stage, the animals were exposed to a new object. The novel and familiar objects exploration time were 2 and 24 h after the familiarization stage. The results indicate that STMR and LTMR recognition indexes diminished in control aging (17.6 % and 33.7 %) and MV (22.8 % and 37.8 %) groups versus the control young adult group ($P < 0.01$; $F = 15.07$). Meanwhile, DV, Metf, and MetfDeca treatments were not statistically different from the control young adult group. STMR and LTMR indexes increased significantly in the animals treated with DV (28 % and 16 %;), Metf (19 % and 20 %), and MetfDeca (21 % and 27 %) compared to the control aging group ($P < 0.0001$; $F = 28.4$). The MV treatment did not show significant changes in the recognition index compared to the control aging group (Fig. 2C - D).

3.2. *Effect of treatments on redox biomarkers in the hippocampus of aged rats*

The oxidative status was evaluated by ROS and LPO quantification in the Hp of the experimental groups (Fig. 3A and 3B). ROS was significative increased in control aging (61.7 %) and MV (73.3 %) groups compared to the control young adult group ($P < 0.0001$; $F = 53.3$), while DV, Metf, and MetfDeca groups were not different. Additionally, LPO was significative augmented in control aging (168.2 %), MV (189.5 %), DV (99.2 %), Metf (94.1 %), and MetfDeca (77.5 %) groups compared to the control young adult group ($P < 0.0001$; $F = 32.3$).

On the other hand, ROS and LPO levels in the control aging and MV groups were not statistically different. However, in DV, Metf, and MetfDeca groups, the hippocampal ROS and LPO concentrations significantly decreased in 38 %, 36 %, and 39 % ($P < 0.0001$; $F = 50.2$), and 25 %, 28 %, and 34 % ($P < 0.0001$; $F = 21.2$), respectively, regarding aging control group.

The anti-oxidant biomarkers analyzed were SOD and CAT activity. The hippocampal SOD activity was significatively decreased in control aging (33.4 %) and MV (34.5 %) groups versus the control young adult group ($P < 0.0001$; $F = 18.5$), while DV, Metf, and MetfDeca groups did not show differences. DV, Metf, and MetfDeca treatments significantly increased SOD activity by 41 %, 39 %, and 75 % regarding the control aging group ($P < 0.0001$; $F = 36.7$; Fig. 3C). Likewise, low CAT activity was shown in control aging (41 %), MV (41.7 %), DV (17.4 %), and Metf (17.8 %) regarding the control young adult group ($P < 0.0001$; $F = 38.8$), while MetfDeca group was not different. A significant increase was observed in the DV (42 %), Metf (41 %), and MetfDeca (73 %) groups regarding the control aging ($P < 0.0001$; $F = 26.3$; Fig. 3D).

We also analyzed the immunoreactivity of Nrf2 as a transcription factor that plays a key role in maintaining anti-oxidative defense. Fig. 4A shows the experimental group photomicrographs from the hippocampal CA1, CA3, and dental gyrus (DG) regions. In the CA1 region (Fig. 4B), the Nrf2 immunoreactivity observed in control young adult group was 1 $\pm$ 1 cells per field, while control aging and MV groups show a significatively increase by 8 $\pm$ 2 and 6 $\pm$ 3 cells per field ($P < 0.0001$; $F =$

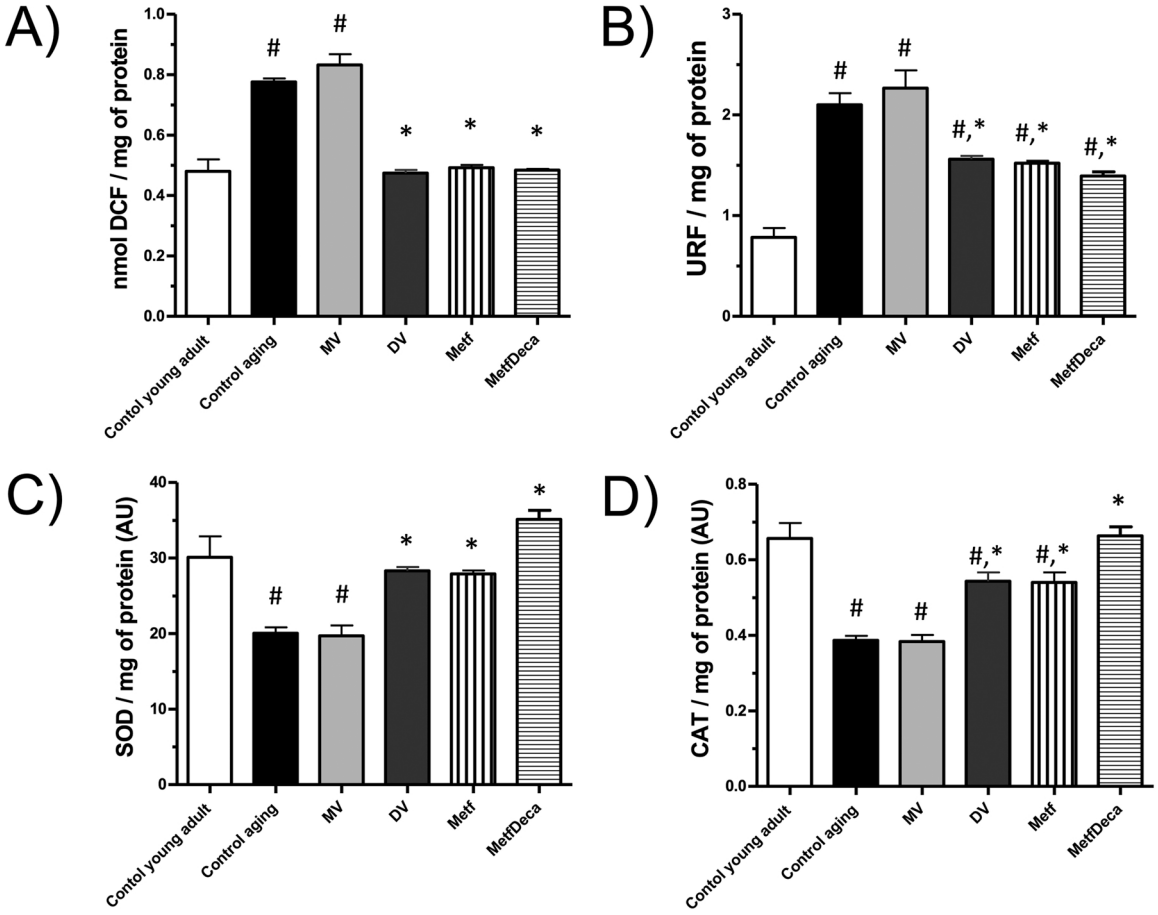

Fig. 3. Redox balance in the hippocampus of rats aging. The redox balance was performed by (1) Control young adult; (2) Control aging; (3) MV (metavanadate); (4) DV (decavanadate); (5) Metf (Metformin); and (6) MetfDeca. Data are reported as mean $\pm$ standard error of the mean (SEM; n = 4 per group). (a) ROS assay; (b) Lipid peroxidation assay; (c) Superoxide activity test; and (d) Catalase activity assay. A two-way ANOVA test was used to analyze the vanadium treatment interaction on aging as independent variables, and a Bonferroni post-test was used to analyze significant differences ($P < 0.05$). (*) Indicates significant differences from the control aging group. (#) Significant differences from the control young adult group.

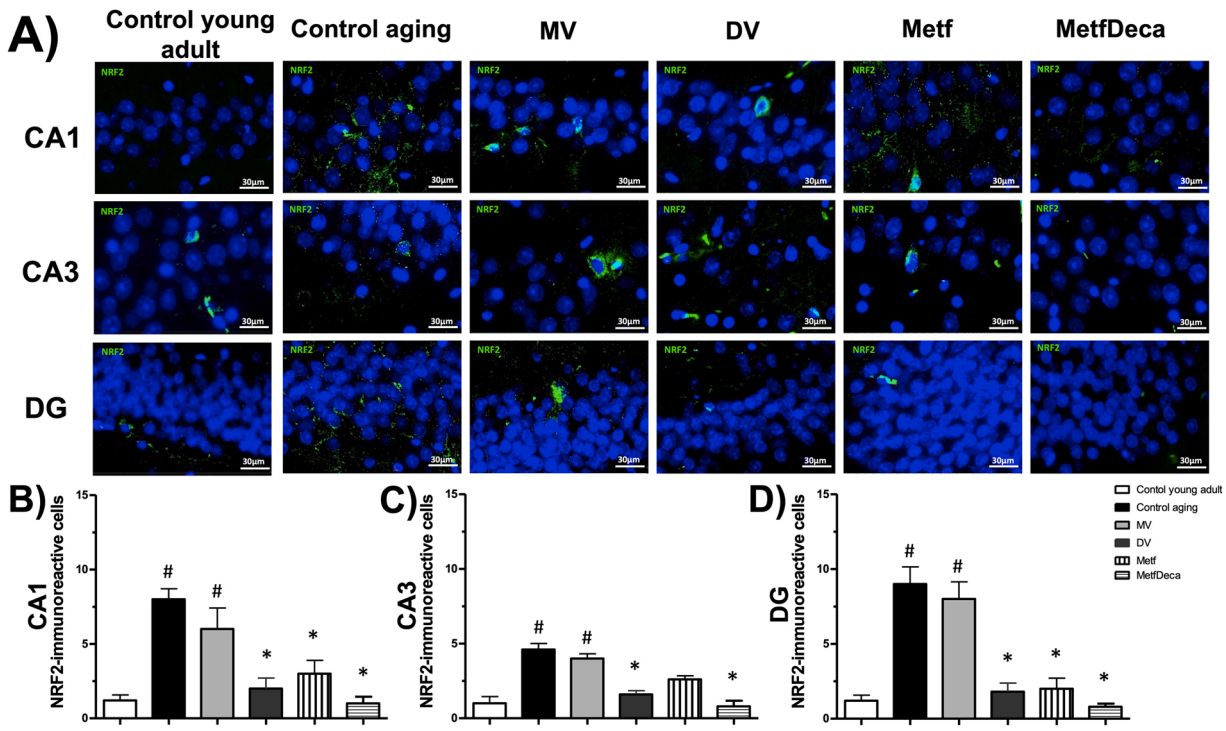

Fig. 4. Nrf2 expression in the hippocampal subregions. The Nrf2 expression was performed by (1) Control young adult; (2) Control aging; (3) MV (metavanadate); (4) DV (decavanadate); (5) Metf (Metformin); and (6) MetfDeca. Data are reported as mean ± standard error of the mean (SEM; n = 4 per group). (a) Photomicrographs of cell immunoreactivity to Nrf2; control young adult (red color), for the rest of the groups (green color), DAPI (nuclei in blue color) in the CA1-CA3-DG subfields of hippocampi; (b) Number of immunoreactive cells (24,975 μm^2). A two-way ANOVA test was used to analyze the vanadium treatment interaction on aging as independent variables, and a Bonferroni post-test was used to analyze significant differences ($P < 0.05$). (*) Indicates significant differences from the control aging group. (#) Significant differences from the control young adult group.

11.3), whereas DV, Metf, and MetfDeca groups showed an average by 2 ± 2, 3 ± 2, and 1 ± 1 cell per field that were not statistically different. Regarding the control aging group, MV treatment was not different, while DV, Metf, and MetfDeca groups significative diminished the number of Nrf2 immunoreactive cells by 75 %, 62.5 %, and 87.5 % ($P < 0.0001$; $F = 23.5$). The control young adult group showed in the CA3 region (Fig. 4 C) an average of 1 ± 1 Nrf2 immunoreactive cells per field, while control aging and MV groups show a significatively increase by 5 ± 1 and 4 ± 1 cell per field ($P < 0.05$; $F = 19.6$), whereas, in the DV, Metf, and MetfDeca groups, the average was 2 ± 1, 3 ± 1, and 1 ± 1 cell per field, without statistical difference. Regarding the control aging group, MV treatment was not different, while DV, Metf, and MetfDeca groups significative diminished the number of Nrf2 immunoreactive cells by 60 %, 40 %, and 80 % ($P < 0.01$; $F = 13.8$). Finally, the control young adult group showed in DG (Fig. 4D) an average of 1 ± 1 Nrf2 immunoreactive cells per field, while control aging and MV groups showed a significative increase by 9 ± 3 and 8 ± 3 cell per field ($P < 0.0001$; $F = 25.6$), whereas DV, Metf, and MetfDeca groups showed an average by 2 ± 2, 2 ± 2, and 1 ± 1 cell per field, without statistical difference. In this region, the MV group was not different from the aging control group. DV, Metf, and MetfDeca groups significantly diminished the number of Nrf2 immunoreactive cells by 78 %, 78 %, and 89 % regarding the aging control group ($P < 0.01$; $F = 16.7$).

3.3. *Effect of treatments on neuroinflammation in the hippocampus of aged rats*

In brain aging, neuroinflammation is observed in the rat hippocampus. The intense immunoreactivity of GFAP in Hp represents the first approach to evidence of the cerebral inflammatory response in aging (Fig. 5A). In the CA1 (Fig. 5B), the control young adult group showed an average of 2 ± 1 immunoreactive cell per field, and the astrocyte number significatively increased in control aging and MV groups by 17 ± 3 and 16 ± 4 cells per field ($P < 0.0001$; $F = 62.7$). At the same time, this parameter was not different in DV, Metf, and MetfDeca groups regarding the control young adult group. DV, Metf, and MetfDeca treatments significatively diminished the number of reactive astrocytes regarding the control aging group in the CA1 by 70 %, 76.5 %, and 82 %, respectively ($P < 0.0001$; $F = 39.9$). In the CA3 (Fig. 5C), the control young adult group, the reactive astrocyte average was 3 ± 1 cells per field, while the control aging and MV groups showed a significative increase by 10 ± 5 and 11 ± 4 cells per field ($P < 0.01$; $F = 13.1$), and DV, Metf, and MetfDeca groups were not different. At the same time, DV, Metf, and MetfDeca treatments significatively diminished the number of reactive astrocytes regarding the control aging group in the CA3 by 60 %, 50 %, and 70 % ($P < 0.05$; $F = 9.5$). In the DG region (Fig. 5D), the reactive astrocyte average in the control young adult group was 4 ± 1 cells per field, observing a significative increase in the control aging and MV groups 14 ± 2 and 16 ± 4 cells per field ($P < 0.001$; $F = 33.8$), but without statistical difference in DV, Metf, and MetfDeca groups. Regarding the control aging group, the DV, Metf, and MetfDeca treatments significatively diminish the number of reactive astrocytes by 57 %, 43 %, and 71 % ($P < 0.05$; $F = 10.4$).

Additionally, we quantified the concentration of IL-1β and TNF-α in the Hp of experimental groups (Fig. 6A - B). The results showed a significant increase in control aging (70 % and 78 %) and MV (74.5 % and 80.4 %) groups, regarding the control young adult group ($P < 0.0001$; $F = 46.5$), but the groups treated with DV, Metf, and MetfDeca were not statically different. Meanwhile, a significant decrease was observed in the DV (40 % and 21.5 %), Metf (40 % and 23 %), and MetfDeca (45 % and 30 %) groups compared to the aging control group ($P < 0.0001$; $F = 35.1$).

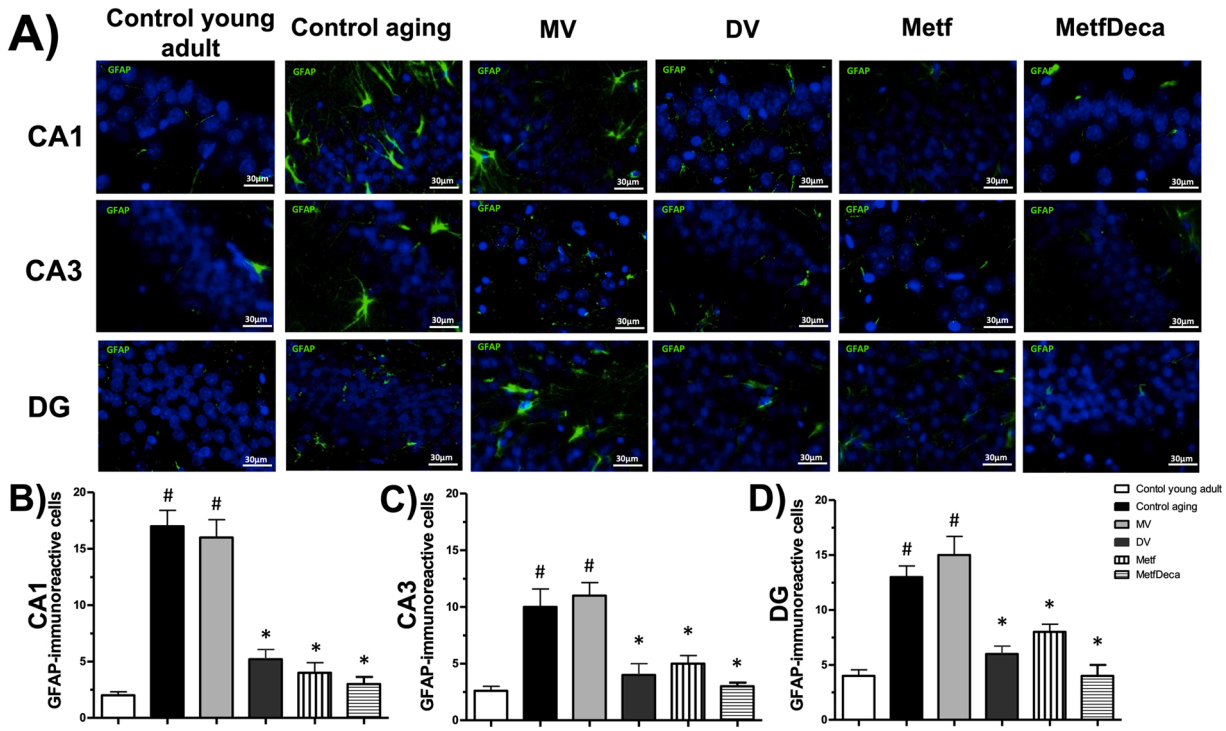

Fig. 5. GFAP expression in the hippocampal subregions. The GFAP expression was performed by (1) Control young adult; (2) Control aging; (3) MV (metavanadate); (4) DV (decavanadate); (5) Metf (Metformin); and (6) MetfDeca. Data are reported as mean ± standard error of the mean (SEM; n = 4 per group). (a) Photomicrographs of cell immunoreactivity to GFAP (green color) and DAPI (nuclei in blue color) in the CA1-CA3-DG subfields of hippocampi; (b) Number of immunoreactive cells (24,975 µm^2). A two-way ANOVA test was used to analyze the vanadium treatment interaction on aging as independent variables, and a Bonferroni post-test was used to analyze significant differences ($P < 0.05$). (*) Indicates significant differences from the control aging group. (#) Significant differences from the control young adult group.

4. Discussion

Aging is a universal, intrinsic, progressive, and multifactorial degenerative process. Different theories have tried to explain the causes of this process. One of the most accepted is the free radical theory of aging. This theory postulates that aging results from deteriorated protective mechanisms that counter oxidative stress damage. Chronically, oxidative stress results in inflammation, immune defects, and cell damage (Johnson et al., 2019; Pomatto and Davies, 2018; Viña, 2019). Currently, the therapeutic strategies are based on caloric restriction, limited amounts of some nutrients, consumption of phytochemicals, such as polyphenols, phytosterols, carotenoids, terpenoids, etc., vitamin and mineral supplementation, such as ascorbic acid or vitamin C, tocopherols like vitamin E, carotenoids, zinc, magnesium, calcium, and some essential polyunsaturated fatty acids (Cummings and Lamming, 2017; Jodynis-Liebert and Kujawska, 2020; Pal and Badireenath Konkimalla, 2016). The pharmacological approaches focus on anti-inflammatory, neurotrophins, and metabolic treatments (Flores et al., 2020). Our workgroup has reported that POVs act on multiple signaling pathways, improving the metabolic status and redox balance in central and peripheral tissues (Diaz et al., 2021; Treviño and González-Vergara, 2019). Therefore, in this study, we investigated if POVs administration positively impacts oxidative stress and inflammation in the hippocampus of aging Wistar rats.

4.1. POVs and Metformin treatments improve age-memory loss

The locomotor and memory alterations linked to age have been observed in rats 18 and 22 months of age (Aguilar-Hernández et al., 2020; Tomm et al., 2018). The reduction in locomotor activity has been related to changes in the structure of the basal ganglia, caudate, putamen, and nucleus accumbens (Aguilar-Hernández et al., 2020; Flores et al., 2016). However, the hippocampus processes and distributes spatial information and behavioral response to contribute to goal-directed trajectory planning from *cornu ammonis* (CA) regions (Luo et al., 2011; Wirtshafter and Wilson, 2019). Our results showed that aging reduces locomotor and exploration activity, and treatments are ineffective in improving them (Fig. 2A-B). In previous reports, rats with metabolic syndrome observed locomotor training improved after two months of Metformin or MetfDeca treatment (Diaz et al., 2021; Muñoz-Arenas et al., 2020).

Our results also showed that learning and memory processes are significantly reduced in aged animals compared to young animals (Arias-Cavieres et al., 2017; Tomm et al., 2018). The hippocampal aging commonly results in defective Ca^{2+} signaling and oxidative stress, leading to significant neuronal function perturbations, glutamatergic synaptic transmission deficits, impairment of long-term potentiation (LTP), and cognitive decline (Arias-Cavieres et al., 2017). However, POVs and Metformin treatments recover the STRM at the same level as the control young adults, showing a high interaction in aging animals (Fig. 2C). Meanwhile, vanadate salt has not demonstrated an effect. The slow decomposition kinetics of POVs (≈11 h) can generate smaller oxidovanadate species with biological activity, which improve cell functions, inflammation, and balance redox (Silva-Nolasco et al., 2020). These results agree with previous reports (Diaz et al., 2021; Muñoz-Arenas et al., 2020), where improvement in recognition memory is linked to reducing cerebral oxidative stress, which has been reported as one of the factors contributing to the neurodegeneration and death of hippocampal neurons (Diaz et al., 2018).

On the other hand, LTRM does not reach the capacity shown by the young controls. Results demonstrated a significant difference but a low interaction of treatment and age regarding LTRM. Probably, POVs and Metformin ameliorated synaptic communication, maintenance of neural structures, and cell death reduction; however, more studies must be

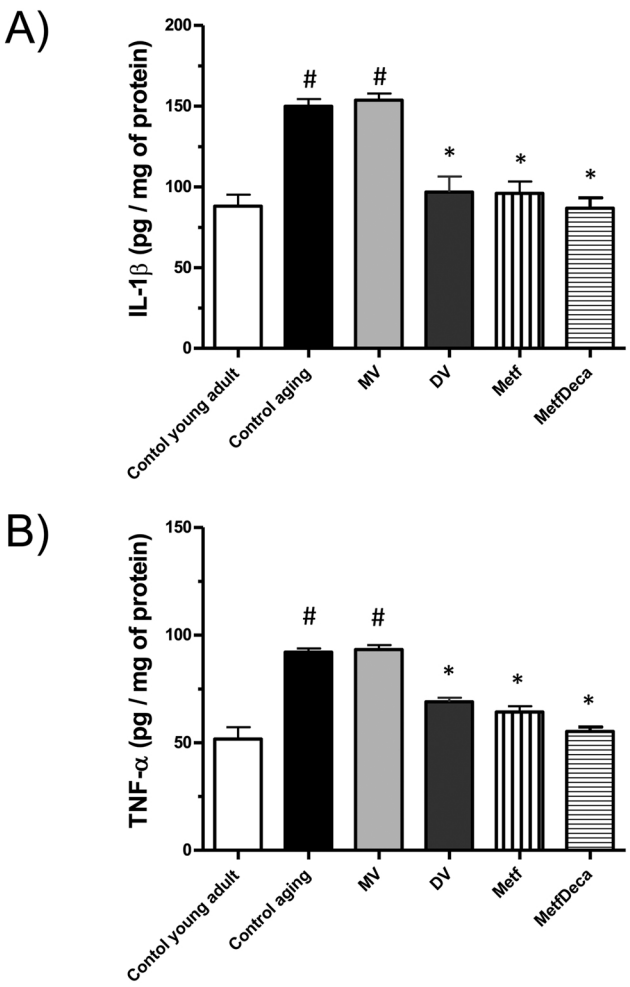

Fig. 6. Inflammaging in the hippocampus of rats aging. The inflammation was performed by (1) Control young adult; (2) Control aging; (3) MV (metavanadate); (4) DV (decavanadate); (5) Metf (Metformin); and (6) MetfDeca. Data are reported as mean ± standard error of the mean (SEM; n = 4 per group). (a) IL-1β; (b) TNF-α. A two-way ANOVA test was used to analyze the vanadium treatment interaction on aging as independent variables, and a Bonferroni post-test was used to analyze significant differences ($P < 0.05$). (*) Indicates significant differences from the control aging group. (#) Significant differences from the control young adult group.

conducted on this matter (Starkman et al., 2003). Metformin and MetfDeca treatments have been demonstrated to improve the neural morphology of hippocampal regions, CA1, CA3, and DG (Diaz et al., 2021; Muñoz-Arenas et al., 2020). Particularly, Metformin administration increases synaptophysin and brain neurotrophic factors, which are associated with recovery of the branching order and dendritic spine density (Muñoz-Arenas et al., 2020). Morphological changes in hippocampal aging have been related to oxidative stress and inflammatory processes (Quinones et al., 2020; Valdés-Ferre et al., 2020). Harman, in 1956 postulated that aging and age-associated degenerative diseases are a consequence of free radical attacks on cells and tissues (Viña, 2019). Oxidative stress induces lipid peroxidation and damages proteins and DNA, altering multiple organelles structurally (Pomatto and Davies, 2018).

4.2. POVs and Metformin treatments improve hippocampal redox balance

Hippocampal ROS and LPO levels increased in a time-dependent manner, and a strong interaction was observed regarding the age variable. Although MV treatment did not show a positive effect on hippocampal oxidative stress, POVs and Metformin treatments diminished hippocampal ROS after two months at the level of young adult control (Fig. 3A). Statistical analysis demonstrated that independent variable "treatments" had the higher interaction ($F = 50.3$) in this study. For therapy with salts or vanadium compounds, it is a general rule that the administration must be below 0.01×10^{-3} M. A concentration above 1.0×10^{-3} M could have toxic effects (Jakusch and Kiss, 2017; Treviño et al., 2019; Treviño and Diaz, 2020). Although the effective therapeutic dose of POVs has not yet been established, it is known that route, concentration, time of administration, and the speciation of the metal are determinants. In voluntary supplementation, vanadium occurs mainly as vanadyl (V^{4+}) or vanadate (V^{5+}) (Thompson and Orvig, 2006).

Meanwhile, POVs such as DV and MetfDeca are slowly biotransformed to vanadate since the pH and oxidative environment generated by aging favor the speciation. Several studies have shown that high ROS, H_2O_2, and superoxide anion ($\bullet O_2^-$) over-generated in mitochondria or NADPH complex carry hydrolytic degradation of POVs to vanadate. In this sense, POVs have excellent stability and biodistribution that permit them to exert their biological functions in less accessible tissues such as the brain instead of vanadate salts, which are biotransformed to V^{4+} species into the liver. Decavanadate and MetfDeca have been shown to diminish mitochondrial $\bullet O^{2-}$ and prevent ROS (Aureliano, 2011; Treviño and González-Vergara, 2019). However, the mechanisms are still unclear. Likewise, Metformin treatment can prevent neurodegenerative disorders associated with oxidative stress (Algire et al., 2012). Some studies have shown the beneficial effects of Metformin in age-related diseases, recommending its administration even in nondiabetic individuals (Gorgich et al., 2021; Ng et al., 2014; Shi et al., 2019; Zhao et al., 2019). However, MetfDeca, as a chimeric compound, offers beneficial activity described to both POVs and Metformin in lower doses, which prevents toxic effects.

Excessive ROS can generate LPO, and the hippocampus is susceptible to structural and DNA damage caused by LPO accumulation (Ferrer et al., 2017). Malondialdehyde (MDA) and 4- hydroxy-2-nonenal (HNE) are major LPO species (Casañas-Sánchez et al., 2015; Song et al., 2021). High MDA, HNE, and HNE-modified proteins are present in the senile plaques in Alzheimer's disease (Echtay et al., 2003). These findings support the hypothesis that LPO contributes to the deterioration of CNS function. Our results confirmed that a high level of hippocampal LPO is strongly associated with aging ($F = 32.3$; Fig. 3B). The metavanadate administration did not improve this damage biomarker. Meanwhile, DV, Metformin, and MetfDeca treatments reduced LPO levels ($F = 21.1$; Fig. 3B). As discussed previously, by diminishing ROS levels, lipid peroxidation decreases. However, the anti-oxidant defense also plays a critical role in preventing neural damage. The robust cell protection is exerted by SOD and CAT activity. The aging significantly decreases the hippocampal activity of both enzymes. Decavanadate and Metformin treatments improved CAT activity; even SOD activity was similar to the control in young adults. However, MetfDeca treatment observed the best anti-oxidant enzyme activity in the hippocampi of aging rats (Fig. 3C - D). Statistical analysis demonstrated a predominant interaction of treatments above age. Additionally, we analyzed the Nrf2 expression because it is a transcriptional factor that senses oxidative stress and modulates balance redox. Nrf2 triggers the transcription of phase II detoxification enzymes and anti-oxidants, such as heme oxygenase 1, γ-glutamylcysteine synthetase, glutathione S-transferase, CAT, and SOD (Cui et al., 2017). Interestingly, control-aging and MV groups observed more immunoreactive cells in CA1, CA3, and DG regions than in young adult rats, possibly as a mechanism to avoid, at least in part, neural damage. POVs and Metformin treatments diminish Nrf2 immunoreactivity in the hippocampal regions studied. However, CA1 showed higher treatment interaction ($F = 23.5$; Fig. 4B), followed by DG ($F = 16.7$; Fig. 4C) and CA3 ($F = 13.8$; Fig. 4D). This behavior may be related to the expression pattern that mainly appears in the cytoplasm around the nucleus (Fig. 4A). Hence, it would be interesting to delve into the study of this pathway to establish precise mechanisms of Metformin and POV

treatments.

A few studies have explored Nrf2 after vanadium treatment. Kim et al. observed that in liver culture cells, treatment with vanadyl sulfate induced the nuclear translocation and accumulation of active Nrf2, presumably mediated by the phosphorylation activity of extracellular signal-regulated kinase (ERK) (Kim et al., 2011). Contrarily, the Ścibior workgroup reported that sodium metavanadate administration in a rodent model led to an increase in MDA in erythrocytes, kidneys, and liver (Ścibior et al., 2018, 2010, 2009). It also attenuated anti-oxidant defense mechanisms by oxidative stress mechanisms. Still, elevated Nrf2 levels were observed (Ścibior et al., 2021). Previously, we reported that after 2 months of administration of sodium metavanadate in a type 1 diabetes model, alloxan induction did not improve Nrf2 expression in the liver, but it did in muscle. Meanwhile, MetfDeca treatment improved Nrf-2 regulation in both tissues, even before insulin treatment. MetfDeca treatment also enhanced the SOD and CAT activity and GSH levels, reducing oxidative stress and LPO biomarkers more effectively than insulin treatment (Treviño and González-Vergara, 2019). In a model of hippocampal senescence induced by metabolic syndrome, MetfDeca treatment ameliorated oxidative damage and activity of anti-oxidant enzymes, possibly via Nrf2. In the present study, our results suggest that in hippocampal regions, Nrf2 regulation is finely controlled by oxidative environmental and corepressors of Keap1-Nerf signaling, which declines during aging (Rahman et al., 2013). Furthermore, recent evidence supports the role of Nrf2 signaling in controlling energy metabolism (Ishii et al., 2018). Therefore, Nrf2 has critical functions for maintaining tissue integrity. Nrf2 can be upregulated via adenosine 5′-monophosphate-activated protein kinase (AMPK) (Yu et al., 2020). AMPK is a cellular energy sensor that regulates energy balance and caloric intake energy, and it is a molecular target of Metformin treatment. Therefore, the AMPK pathway is neuroprotective. Hippocampal overexpression has been reported in rodent models of metabolic syndrome and acute stroke patients with type 2 diabetes (Muñoz-Arenas et al., 2020; Yu et al., 2020; Zhao et al., 2019).

4.3. POVs and metformin treatments reduce hippocampal inflammation

Redox-sensitive transcription factors such as nuclear factor kappa B (NF-κB) are activated by ROS, inducing the expression of inflammatory proteins, such as tumor necrosis factor-alpha (TNF-α), interleukins (IL-1β and −6), mainly by reactive microglia (Sivandzade et al., 2019). The ROS and inflammatory signaling are redundant and accentuate with age. Therefore, increasing evidence associates aging and age-related diseases with oxidative stress and inflammation (Diaz et al., 2018; Flores et al., 2016; Ruíz-Salinas et al., 2020). Inflammaging is an inflammatory response of low-grade, slow, chronic upregulation, which is progressive in the aging brain, causing neurobiological modifications (Deleidi et al., 2015). The inflammation affects most of the CNS, particularly the hippocampus, that when impaired, leads to deficient cognitive functions. Our results showed more elevated IL-1β and TNF-α concentrations in control aging and MV groups than in young-adult rats, with high interaction ($F = 46.5$). Meanwhile, groups administered with DV, Metformin, and MetfDeca significantly diminished IL-1β and TNF-α at the level of a younger rat (Fig. 6A – B). Vanadium compounds have demonstrated that they inactivate NF-κB and decrease inflammation (Gallardo-Vera et al., 2018; Semiz, 2022; Tsave et al., 2016). Likewise, MetfDeca treatment also reduces pro-inflammatory cytokines in the hippocampus of rats with metabolic syndrome (Diaz et al., 2021). Metformin treatment also reduces inflammation by activating the AMPK/Silent information regulator T1 (Sirt1) pathway (Chen et al., 2020). Sirt1 is an NAD^+-dependent histone deacetylase, playing diverse roles in stress resistance, apoptosis, senescence, aging, and inflammation. Sirt1 diminishes concentration and inhibits NF-κB activity, hence the inflammation (de Gregorio et al., 2020). The POVs could modulate inflammation of both ERK and NF-κB pathways, while MV treatment has the opposite effect (Tsave et al., 2016).

Evidence demonstrates that inflammation and lack of microglial and/or astrocyte support are responsible for neuronal degeneration (Lana et al., 2021). Microglia in normal aging upregulate immune, pro-inflammatory responses, and neuroprotective signaling pathways, which could promote the activation of astrocytes (Grabert et al., 2016; Liddelow and Barres, 2017). Astrocyte overactivity, namely astrocytosis, is characterized by a significant increase in GFAP expression, which correlates with our results. Control aging and MV groups observed more intense immunoreaction to GFAP in CA1, CA3, and DG than in the control young adult group (Fig. 5A). GFAP demonstrated the most interaction regarding age in CA1 ($F = 62.7$), DG ($F = 33.8$), and CA3 ($F = 13.1$); thereby, results indicate that it could be the neurodegenerative order in the hippocampal regions. GFAP, inflammation, and oxidative stress were associated with aging, as in other works (Clarke et al., 2018; Middeldorp and Hol, 2011). Rodents were found to have more reactive/activated astrocytes, although they are not more numerous (Burda and Sofroniew, 2014; Liddelow and Barres, 2017). However, GFAP reactivity diminished after administering DV, Metformin, and MetfDeca (Fig. 5B - D). Treatments improve astrocytosis in the same order that aging affects the hippocampal regions, with a high interaction in CA1 ($F = 39.9$) and a low interaction in DG ($F = 10.4$) and CA3 ($F = 9.5$). These findings are a novelty because, to our knowledge, there are no previous reports of this. The improvement observed by POVs and Metformin treatments is congruent with cognitive function recovery. In this way, the MetfDeca administration has also reported amelioration of neuronal features in hippocampal subregions. Meanwhile, Bis (ethylmaltolato) oxidovanadium (BEOV) administration in a transgenic model mouse with Alzheimer's disease (AD) decreased the time to find the platform in the Morris Water Maze, the generation of Amyloid-β peptide (Aβ), tau hyperphosphorylation and β-secretase1 in the hippocampus and cortex. Dong et al. observed cognitive function preservation and attenuation of neuron loss after administrating vanadyl (IV) acetylacetonate (0.1 mmol/kg/day) in AD in vitro and in vivo models. However, it did not reduce the Aβ plaques (Diaz et al., 2021).

5. Conclusion

In summary, cognitive functions, such as learning and memory processes, were reduced in aged animals. These alterations were associated with oxidative stress and inflammaging in the hippocampus, linked to astrocytosis in the CA1, CA3, and DG subregions. After administrating oral dosages of MV, DV, Metformin, and MetfDeca to 18-month rats for two months, MV treatment did not modify oxidative stress, inflammation, and astrocytosis; hence it did not enhance the STRM and LTMR. Meanwhile, treatments with DV, Metformin, and MetfDeca ameliorate all parameters evaluated. Our results suggest that POVs and Metformin finely regulate Nrf2, a key redox balance sensor in hippocampal regions, which improves anti-oxidant defense, reduces oxidative stress and inflammation biomarkers, and prevents age-cognitive function loss. Remarkably, the POV dosages were 16-fold lower and more effective than the Metformin dose. In conclusion, decavanadate and metforminium-decavanadate could be pharmacological options to reduce aging-associated neuronal damage.

Funding

This work was supported by grants from Vicerrectoria de Investigación y Posgrado of Benemérita Universidad Autónoma de Puebla [VIEP; TRMS-NAT22–1].

CRediT authorship contribution statement

All authors contributed to the study conception and design. Material preparation, data collection and analysis were performed by **Samuel Treviño**, **Alfonso Díaz**, **Karen Carreto-Meneses**, **Diana Moroni-González** and **José Albino Moreno-Rodríguez**. The first draft of the

manuscript was written by **Samuel Treviño** and all authors commented on previous versions of the manuscript. All authors read and approved the final manuscript.

Conflict of interest statement

The authors declare that the research was conducted in the absence of any commercial or financial relationships that could be construed as a potential conflict of interest.

Acknowledgments

The authors thank Vicerrectoria de Investigación y Posgrado of Benemérita Universidad Autónoma de Puebla [VIEP; TRMS-NAT22–1] through Ygnacio Martínez Lagunaand Dr. Francisco Ramos Collazo (Bioterio "Claude Bernard," BUAP) for his assistance and the donation of the animals used in this study. We also express our gratitude to Dra. Yhisell Domínguez Alonso of the Clinical Laboratory "CAISS S.A de C.V" for the facilities to carry out this study. We thank Professor Robert Simpson for editing the English language text.

Ethical Statement

The procedures described in this study were approved by the CICUAL-BUAP ethics committee for animal handling and performed according to the guide for the care and use of laboratory animals: NOM-062-ZOO-1999. All applicable international, national, and institutional guidelines for the care and use of animals were followed to minimize possible discomfort.

References

Aguilar-Hernández, L., Vázquez-Hernández, A.J., De-Lima-Mar, D.F., Vázquez-Roque, R. A., Tendilla-Beltrán, H., Flores, G., 2020. Memory and dendritic spines loss, and dynamic dendritic spines changes are age-dependent in the rat. J. Chem. Neuroanat. 110, 101858 https://doi.org/10.1016/J.JCHEMNEU.2020.101858.

Alexander, G.E., Ryan, L., Bowers, D., Foster, T.C., Bizon, J.L., Geldmacher, D.S., Glisky, E.L., 2012. Characterizing cognitive aging in humans with links to animal models. Front. Aging Neurosci. 4 https://doi.org/10.3389/FNAGI.2012.00021.

Algire, C., Moiseeva, O., Deschênes-Simard, X., Amrein, L., Petruccelli, L., Birman, E., Viollet, B., Ferbeyre, G., Pollak, M.N., 2012. Metformin reduces endogenous reactive oxygen species and associated DNA damage. Cancer Prev. Res. 5, 536–543. https://doi.org/10.1158/1940-6207.CAPR-11-0536.

Arias-Cavieres, A., Adasme, T., Sánchez, G., Muñoz, P., Hidalgo, C., 2017. Aging impairs hippocampal- dependent recognition memory and LTP and prevents the associated RyR up-regulation. Front. Aging Neurosci. 9 https://doi.org/10.3389/FNAGI.2017.00111.

Aureliano, M., 2011. Recent perspectives into biochemistry of decavanadate. World J. Biol. Chem. 2, 215. https://doi.org/10.4331/wjbc.v2.i10.215.

Aureliano, M., 2016. Decavanadate toxicology and pharmacological activities: V10 or v1, both or none? Oxid. Med. Cell. Longev. 2016, 15–17. https://doi.org/10.1155/2016/6103457.

Aureliano, M., 2022. The future is bright for polyoxometalates. BioChem 2, 8–26. https://doi.org/10.3390/BIOCHEM2010002.

Aureliano, M., Ohlin, C.A., Vieira, M.O., Marques, M.P.M., Casey, W.H., Batista De Carvalho, L.A.E., 2016. Characterization of decavanadate and decaniobate solutions by Raman spectroscopy. Dalton Trans. 45, 7391–7399. https://doi.org/10.1039/c5dt04176g.

Aureliano, M., Gumerova, N.I., Sciortino, G., Garribba, E., Mclauchlan, C.C., Rompel, A., Crans, D.C., 2022. Polyoxidovanadates' interactions with proteins: an overview. Coord. Chem. Rev. 454, 214344 https://doi.org/10.1016/J.CCR.2021.214344.

Barja, G., 2013. Updating the mitochondrial free radical theory of aging: an integrated view, key aspects, and confounding concepts. Anti-Oxid. Redox Signal. 19, 1420–1445. https://doi.org/10.1089/ARS.2012.5148.

Barja, G., 2014. The mitochondrial free radical theory of aging. Prog. Mol. Biol. Transl. Sci. 127, 1–27. https://doi.org/10.1016/B978-0-12-394625-6.00001-5.

Burda, J.E., Sofroniew, M.V., 2014. Reactive gliosis and the multicellular response to CNS damage and disease. Neuron 81, 229–248. https://doi.org/10.1016/J.NEURON.2013.12.034.

Casañas-Sánchez, V., Pérez, J.A., Fabelo, N., Quinto-Alemany, D., Díaz, M.L., 2015. Docosahexaenoic (DHA) modulates phospholipid-hydroperoxide glutathione peroxidase (Gpx4) gene expression to ensure self-protection from oxidative damage in hippocampal cells. Front. Physiol. 6 https://doi.org/10.3389/FPHYS.2015.00203.

Chen, Yong, Qiu, F., Yu, B., Chen, Yanjuan, Zuo, F., Zhu, X.Y., Nandakumar, K.S., Xiao, C., 2020. Metformin, an AMPK activator, inhibits activation of FLSs but promotes HAPLN1 secretion. Mol. Ther. Methods Clin. Dev. 17, 1202. https://doi.org/10.1016/J.OMTM.2020.05.008.

Clarke, L.E., Liddelow, S.A., Chakraborty, C., Münch, A.E., Heiman, M., Barres, B.A., 2018. Normal aging induces A1-like astrocyte reactivity. Proc. Natl. Acad. Sci. USA 115, E1896–E1905. https://doi.org/10.1073/PNAS.1800165115/-/DCSUPPLEMENTAL.

Cui, W., Min, X., Xu, X., Du, B., Luo, P., 2017. Role of nuclear factor erythroid 2-related factor 2 in diabetic nephropathy. J. Diabetes Res. 2017. https://doi.org/10.1155/2017/3797802.

Cummings, N.E., Lamming, D.W., 2017. Regulation of metabolic health and aging by nutrient-sensitive signaling pathways. Mol. Cell. Endocrinol. 455, 13. https://doi.org/10.1016/J.MCE.2016.11.014.

Deleidi, M., Jäggle, M., Rubino, G., 2015. Immune aging, dysmetabolism, and inflammation in neurological diseases. Front. Neurosci. 9, 172. https://doi.org/10.3389/FNINS.2015.00172.

Diaz, A., Escobedo, C., Treviño, S., Chávez, R., Lopez-Lopez, G., Moran, C., Guevara, J., Venegas, B., Muñoz-Arenas, G., 2018. Metabolic syndrome exacerbates the recognition memory impairment and oxidative-inflammatory response in rats with an intrahippocampal injection of amyloid beta 1-42. Oxid. Med Cell Longev. 2018, 1358057. https://doi.org/10.1155/2018/1358057.

Diaz, A., Muñoz-Arenas, G., Venegas, B., Vázquez-Roque, R., Flores, G., Guevara, J., Gonzalez-Vergara, E., Treviño, S., 2021. Metforminium decavanadate (MetfDeca) treatment ameliorates hippocampal neurodegeneration and recognition memory in a metabolic syndrome model. Neurochem Res. 46, 1151–1165. https://doi.org/10.1007/S11064-021-03250-Z/FIGURES/6.

Dykiert, D., Der, G., Starr, J.M., Deary, I.J., 2012. Age differences in intra-individual variability in simple and choice reaction time: systematic review and meta-analysis. PLOS One 7. https://doi.org/10.1371/JOURNAL.PONE.0045759.

Echtay, K.S., Esteves, T.C., Pakay, J.L., Jekabsons, M.B., Lambert, A.J., Portero-Otín, M., Pamplona, R., Vidal-Puig, A.J., Wang, S., Roebuck, S.J., Brand, M.D., 2003. A signalling role for 4-hydroxy-2-nonenal in regulation of mitochondrial uncoupling. EMBO J. 22, 4103–4110. https://doi.org/10.1093/EMBOJ/CDG412.

Ferrer, I., Gil-Villar, M.P., Ayala, V., Jové, M., Mota-Martorell, N., Portero-Otín, M., Pamplona, R., 2017. Region-specific vulnerability to lipid peroxidation and evidence of neuronal mechanisms for polyunsaturated fatty acid biosynthesis in the healthy adult human central nervous system. Biochim. Biophys. Acta Mol. Cell Biol. Lipids 1862, 485–495. https://doi.org/10.1016/J.BBALIP.2017.02.001.

Flores, G., Vázquez-Roque, R.A., Diaz, A., 2016. Resveratrol effects on neural connectivity during aging. Neural Regen. Res. 11, 1067–1068. https://doi.org/10.4103/1673-5374.187029.

Flores, G., Flores-Gómez, G.D., Díaz, A., Penagos-Corzo, J.C., Iannitti, T., Morales-Medina, J.C., 2020. Natural products present neurotrophic properties in neurons of the limbic system in aging rodents. Synapse 75. https://doi.org/10.1002/SYN.22185.

Foroushani, A.R., Estebsari, F., Mostafaei, D., Ardebili, H.E., Shojaeizadeh, D., Dastoorpour, M., Jamshidi, E., Taghdisi, M.H., 2014. The effect of health promoting intervention on healthy lifestyle and social support in elders: a clinical trial study. Iran. Red. Crescent Med. J. 16, 18399 https://doi.org/10.5812/IRCMJ.18399.

Gallardo-Vera, F., Tapia-Rodriguez, M., Diaz, D., Fortoul van der Goes, T., Montaño, L.F., Rendón-Huerta, E.P., 2018. Vanadium pentoxide increased PTEN and decreased SHP1 expression in NK-92MI cells, affecting PI3K-AKT-mTOR and Ras-MAPK pathways. J. Immunotoxicol. 15, 1–11. https://doi.org/10.1080/1547691X.2017.1404662.

Gorgich, E.A.C., Parsaie, H., Yarmand, S., Baharvand, F., Sarbishegi, M., 2021. Long-term administration of Metformin ameliorates age-dependent oxidative stress and cognitive function in rats. Behav. Brain Res. 410, 113343 https://doi.org/10.1016/J.BBR.2021.113343.

Grabert, K., Michoel, T., Karavolos, M.H., Clohisey, S., Kenneth Baillie, J., Stevens, M.P., Freeman, T.C., Summers, K.M., McColl, B.W., 2016. Microglial brain region-dependent diversity and selective regional sensitivities to aging. Nat. Neurosci. 19, 504–516. https://doi.org/10.1038/NN.4222.

de Gregorio, E., Colell, A., Morales, A., Marí, M., 2020. Relevance of SIRT1-NF-κB axis as therapeutic target to ameliorate inflammation in liver disease. Int. J. Mol. Sci. 21, 1–24. https://doi.org/10.3390/IJMS21113858.

Isaev, N.K., Stelmashook, E.V., Genrikhs, E.E., 2019. Neurogenesis and brain aging. Rev. Neurosci. 30, 573–580. https://doi.org/10.1515/REVNEURO-2018-0084.

Ishii, T., Warabi, E., Mann, G.E., 2018. Circadian control of p75 neurotrophin receptor leads to alternate activation of Nrf2 and c-Rel to reset energy metabolism in astrocytes via brain-derived neurotrophic factor. Free Radic. Biol. Med. 119, 34–44. https://doi.org/10.1016/J.FREERADBIOMED.2018.01.026.

Jakusch, T., Kiss, T., 2017. In vitro study of the antidiabetic behavior of vanadium compounds. Coord. Chem. Rev. 351, 118–126. https://doi.org/10.1016/j.ccr.2017.04.007.

Jodynis-liebert, J., Kujawska, M., 2020. Biphasic dose-response induced by phytochemicals: experimental evidence. J. Clin. Med. 9 https://doi.org/10.3390/JCM9030718.

Johnson, A.A., Shokhirev, M.N., Shoshitaishvili, B., 2019. Revamping the evolutionary theories of aging. Ageing Res. Rev. 55 https://doi.org/10.1016/J.ARR.2019.100947.

Khan, S.S., Singer, B.D., Vaughan, D.E., 2017. Molecular and physiological manifestations and measurement of aging in humans. Aging Cell 16, 624–633. https://doi.org/10.1111/ACEL.12601.

Kim, A.D., Zhang, R., Kang, K.A., You, H.J., Hyun, J.W., 2011. Increased glutathione synthesis following Nrf2 activation by vanadyl sulfate in human chang liver cells. Int. J. Mol. Sci. 12, 8878. https://doi.org/10.3390/IJMS12128878.

Lana, D., Ugolini, F., Nosi, D., Wenk, G.L., Giovannini, M.G., 2021. The emerging role of the interplay among astrocytes, microglia, and neurons in the hippocampus in health

and disease. Front. Aging Neurosci. 13, 651973 https://doi.org/10.3389/FNAGI.2021.651973.
Levin, O., Fujiyama, H., Boisgontier, M.P., Swinnen, S.P., Summers, J.J., 2014. Aging and motor inhibition: a converging perspective provided by brain stimulation and imaging approaches. Neurosci. Biobehav. Rev. 43, 100–117. https://doi.org/10.1016/J.NEUBIOREV.2014.04.001.
Liang, S., Wu, S., Huang, Q., Duan, S., Liu, H., Li, Y., Zhao, S., Nie, B., Shan, B., 2017. Rat brain digital stereotaxic white matter atlas with fine tract delineation in Paxinos space and its automated applications in DTI data analysis. Magn. Reson. Imaging 43, 122–128. https://doi.org/10.1016/J.MRI.2017.07.011.
Liddelow, S.A., Barres, B.A., 2017. Reactive astrocytes: production, function, and therapeutic potential. Immunity 46, 957–967. https://doi.org/10.1016/J.IMMUNI.2017.06.006.
Luo, A.H., Tahsili-Fahadan, P., Wise, R.A., Lupica, C.R., Aston-Jones, G., 2011. Linking context with reward: a functional circuit from hippocampal CA3 to ventral tegmental area. Science 333, 353–357. https://doi.org/10.1126/SCIENCE.1204622.
Mattson, M.P., Arumugam, T.V., 2018. Hallmarks of brain aging: adaptive and pathological modification by metabolic states. Cell Metab. 27, 1176. https://doi.org/10.1016/J.CMET.2018.05.011.
Middeldorp, J., Hol, E.M., 2011. GFAP in health and disease. Prog. Neurobiol. 93, 421–443. https://doi.org/10.1016/J.PNEUROBIO.2011.01.005.
Muñoz-Arenas, G., Pulido, G., Treviño, S., Vázquez-Roque, R., Flores, G., Moran, C., Handal-Silva, A., Guevara, J., Venegas, B., Díaz, A., 2020. Effects of metformin on recognition memory and hippocampal neuroplasticity in rats with metabolic syndrome. Synapse 74, e22153. https://doi.org/10.1002/SYN.22153.
Nations Department of Economic, U., Affairs, S., Division, P., 2019. World Population Ageing 2019.
Ng, T.P., Feng, L., Yap, K.B., Lee, T.S., Tan, C.H., Winblad, B., 2014. Long-term metformin usage and cognitive function among older adults with diabetes. J. Alzheimer'S. Dis. 41, 61–68. https://doi.org/10.3233/JAD-131901.
Pal, S., Badireenath Konkimalla, V., 2016. Hormetic potential of sulforaphane (SFN) in switching cells' fate towards survival or death. Mini-Rev. Med. Chem. 16, 980–995. https://doi.org/10.2174/1389557516666151120115027.
Perry, W., Lacritz, L., Roebuck-Spencer, T., Silver, C., Denney, R.L., Meyers, J., Mcconnel, C.E., Pliskin, N., Adler, D., Alban, C., Bondi, M., Braun, M., Cagigas, X., Daven, M., Drozdick, L., Foster, N.L., Hwang, U., Ivey, L., Iverson, G., Kramer, J., Lantz, M., Latts, L., Ling, S.M., Maria Lopez, A., Malone, M., Martin-Plank, L., Maslow, K., Melady, D., Messer, M., Most, R., Norris, M.P., Shafer, D., Silverberg, N., Thomas, C.M., Thornhill, L., Tsai, J., Vakharia, N., Waters, M., Golden, T., 2018. Population health solutions for assessing cognitive impairment in geriatric patients. Innov. Aging 2, 1–21. https://doi.org/10.1093/GERONI/IGY025.
Pomatto, L.C.D., Davies, K.J.A., 2018. Adaptive homeostasis and the free radical theory of ageing. Free Radic. Biol. Med. 124, 420–430. https://doi.org/10.1016/J.FREERADBIOMED.2018.06.016.
Quinones, M.M., Gallegos, A.M., Lin, F.V., Heffner, K., 2020. Dysregulation of inflammation, neurobiology, and cognitive function in PTSD: an integrative review. Cogn., Affect. Behav. Neurosci. 20, 455–480. https://doi.org/10.3758/S13415-020-00782-9.
Rahman, M.M., Sykiotis, G.P., Nishimura, M., Bodmer, R., Bohmann, D., 2013. Declining signal-dependence of Nrf2-MafS regulated gene expression correlates with aging phenotypes. Aging Cell 12, 554. https://doi.org/10.1111/ACEL.12078.
Ruíz-Salinas, A.K., Vázquez-Roque, R.A., Díaz, A., Pulido, G., Treviño, S., Floran, B., Flores, G., 2020. The treatment of Goji berry (Lycium barbarum) improves the neuroplasticity of the prefrontal cortex and hippocampus in aged rats. J. Nutr. Biochem. 83 https://doi.org/10.1016/J.JNUTBIO.2020.108416.
Sanz, A., Stefanatos, R.K.A., 2010. The mitochondrial free radical theory of aging: a critical view. Curr. Aging Sci. 1, 10–21. https://doi.org/10.2174/1874609810801010010.
Ścibior, A., Zaporowska, H., Niedźwiecka, I., 2009. Lipid peroxidation in the liver of rats treated with V and/or Mg in drinking water. J. Appl. Toxicol. 29, 619–628. https://doi.org/10.1002/JAT.1450.
Ścibior, A., Zaporowska, H., Niedźwiecka, I., 2010. Lipid peroxidation in the kidney of rats treated with V and/or Mg in drinking water. J. Appl. Toxicol. 30, 487–496. https://doi.org/10.1002/JAT.1520.
Ścibior, A., Adamczyk, A., Gołębiowska, D., Kurus, J., 2018. Evaluation of lipid peroxidation and the level of some elements in rat erythrocytes during separate and combined vanadium and magnesium administration. Chem. -Biol. Interact. 293, 1–10. https://doi.org/10.1016/J.CBI.2018.07.014.
Ścibior, A., Wojda, I., Wnuk, E., Pietrzyk, Ł., Plewa, Z., 2021. Response of cytoprotective and detoxifying proteins to vanadate and/or magnesium in the rat liver: the Nrf2-Keap1 system. Oxid. Med. Cell. Longev. 2021. https://doi.org/10.1155/2021/8447456.
Semiz, S., 2022. Vanadium as potential therapeutic agent for COVID-19: A focus on its antiviral, antiinflamatory, and antihyperglycemic effects. J. Trace Elem. Med. Biol. 69, 126887 https://doi.org/10.1016/J.JTEMB.2021.126887.
Shi, Q., Liu, S., Fonseca, V.A., Thethi, T.K., Shi, L., 2019. Effect of Metformin on neurodegenerative disease among elderly adult US veterans with type 2 diabetes mellitus. BMJ Open 9. https://doi.org/10.1136/BMJOPEN-2018-024954.
Silva-Nolasco, A.M., Camacho, L., Saavedra-Díaz, R.O., Hernández-Abreu, O., León, I.E., Sánchez-Lombardo, I., 2020. Kinetic studies of sodium and metforminium decavanadates decomposition and in vitro cytotoxicity and insulin- like activity. Inorganics 8. https://doi.org/10.3390/INORGANICS8120067.
Sivandzade, F., Prasad, S., Bhalerao, A., Cucullo, L., 2019. NRF2 and NF-κB interplay in cerebrovascular and neurodegenerative disorders: molecular mechanisms and possible therapeutic approaches. Redox Biol. 21 https://doi.org/10.1016/J.REDOX.2018.11.017.
Song, Z., Shah, S., Lv, B., Ji, N., Liu, X., Yan, L., Khan, M., Zhao, Y., Wu, P., Liu, S., Zheng, L., Su, L., Wang, X., Lv, Z., 2021. Anti-aging and anti-oxidant activities of murine short interspersed nuclear element antisense RNA. Eur. J. Pharmacol. 912 https://doi.org/10.1016/J.EJPHAR.2021.174577.
Starkman, M.N., Giordani, B., Gebarski, S.S., Schteingart, D.E., 2003. Improvement in learning associated with increase in hippocampal formation volume. Biol. Psychiatry 53, 233–238. https://doi.org/10.1016/S0006-3223(02)01750-X.
Thompson, K.H., Orvig, C., 2006. Vanadium in diabetes: 100 years from Phase 0 to Phase I. J. Inorg. Biochem. 100, 1925–1935. https://doi.org/10.1016/j.jinorgbio.2006.08.016.
Tomm, R.J., Tse, M.T., Tobiansky, D.J., Schweitzer, H.R., Soma, K.K., Floresco, S.B., 2018. Effects of aging on executive functioning and mesocorticolimbic dopamine markers in male Fischer 344 × brown Norway rats. Neurobiol. Aging 72, 134–146. https://doi.org/10.1016/J.NEUROBIOLAGING.2018.08.020.
Treviño, S., Díaz, A., 2020. Vanadium and insulin: partners in metabolic regulation. J. Inorg. Biochem. https://doi.org/10.1016/j.jinorgbio.2020.111094.
Treviño, S., González-Vergara, E., 2019. Metformin-decavanadate treatment ameliorates hyperglycemia and redox balance of the liver and muscle in a rat model of alloxan-induced diabetes. N. J. Chem. 43, 17850–17862. https://doi.org/10.1039/c9nj02460c.
Treviño, S., Sánchez-Lara, E., Sarmiento-Ortega, V.E., Sánchez-Lombardo, I., Flores-Hernández, J.Á., Pérez-Benítez, A., Brambila-Colombres, E., González-Vergara, E., 2015. Hypoglycemic, lipid-lowering and metabolic regulation activities of metforminium decavanadate (H2Metf)3 [V10O28]·8H2O using hypercaloric-induced carbohydrate and lipid deregulation in Wistar rats as biological model. J. Inorg. Biochem. 147, 85–92. https://doi.org/10.1016/j.jinorgbio.2015.04.002.
Treviño, S., Velázquez-vázquez, D., Sánchez-lara, E., Diaz-, A., Flores-hernandez, J.Á., Pérez-benítez, A., Brambila-, E., González-vergara, E., 2016. Metforminium decavanadate as a potential metallopharmaceutical drug for the treatment of diabetes mellitus. Oxid. Med. Cell. Longev. 2016. https://doi.org/10.1155/2016/6058705.
Treviño, S., Díaz, A., Sánchez-Lara, E., Sarmiento-Ortega, V.E., Flores-Hernández, J.Á., Brambila, E., Meléndez, F.J., González-Vergara, E., 2018. Pharmacological and toxicological threshold of bisammonium tetrakis 4-(N,N-Dimethylamino)pyridinium decavanadate in a rat model of metabolic syndrome and insulin resistance. Bioinorg. Chem. Appl. 2018, 2151079 https://doi.org/10.1155/2018/2151079.
Treviño, S., Díaz, A., Sánchez-Lara, E., Sanchez-Gaytan, B.L., Perez-Aguilar, J.M., González-Vergara, E., 2019. Vanadium in biological action: chemical, pharmacological aspects, and metabolic implications in diabetes mellitus. Biol. Trace Elem. Res. 188, 68–98. https://doi.org/10.1007/s12011-018-1540-6.
Tsave, O., Petanidis, S., Kioseoglou, E., Yavropoulou, M.P., Yovos, J.G., Anestakis, D., Tsepa, A., Salifoglou, A., 2016. Role of vanadium in cellular and molecular immunology: association with immune-related inflammation and pharmacotoxicology mechanisms. Oxid. Med. Cell. Longev. 2016. https://doi.org/10.1155/2016/4013639.
Valdés-Ferre, S.I., Benkendorff, A., Sankowski, R., 2020. Persistent inflammatory states and their implications in brain disease. Curr. Opin. Neurol. 33, 341–346. https://doi.org/10.1097/WCO.0000000000000809.
Viña, J., 2019. The free radical theory of frailty: mechanisms and opportunities for interventions to promote successful aging. Free Radic. Biol. Med. 134, 690–694. https://doi.org/10.1016/J.FREERADBIOMED.2019.01.045.
Wahl, D., Solon-Biet, S.M., Cogger, V.C., Fontana, L., Simpson, S.J., Le Couteur, D.G., Ribeiro, R.V., 2019. Aging, lifestyle and dementia. Neurobiol. Dis. 130. https://doi.org/10.1016/J.NBD.2019.104481.
Wirtshafter, H.S., Wilson, M.A., 2019. Locomotor and hippocampal processing converge in the lateral septum. Curr. Biol. 29 (3177–3192) https://doi.org/10.1016/J.CUB.2019.07.089.
Yu, J., Wang, W.N., Matei, N., Li, X., Pang, J.W., Mo, J., Chen, S.P., Tang, J.P., Yan, M., Zhang, J.H., 2020. Ezetimibe attenuates oxidative stress and neuroinflammation via the AMPK/Nrf2/TXNIP pathway after MCAO in rats. Oxid. Med. Cell. Longev. 2020. https://doi.org/10.1155/2020/4717258.
Zhao, M., Li, X.W., Chen, D.Z., Hao, F., Tao, S.X., Yu, H.Y., Cheng, R., Liu, H., 2019. Neuro-protective role of metformin in patients with acute stroke and type 2 diabetes mellitus via AMPK/mammalian target of rapamycin (mTOR) signaling pathway and oxidative stress. Med. Sci. Monit.: Int. Med. J. Exp. Clin. Res. 25, 2186–2194. https://doi.org/10.12659/MSM.911250.
Zhou, B., Zuo, Y.X., Jiang, R.T., 2019. Astrocyte morphology: Diversity, plasticity, and role in neurological diseases. CNS Neurosci. Ther. 25, 665–673. https://doi.org/10.1111/CNS.13123.